

the Gaussian model eq 35 yields results close to  $\beta_{\text{trad}}$ .

On account of the energy dependence of  $\langle \Delta E \rangle$  in most models, the analogous relation  $\langle \Delta E \rangle = -\langle \Delta E \rangle_{\text{down}} \beta^{1/2}$ , with  $\langle \Delta E \rangle_{\text{down}}$  of eq 35, obviously cannot apply, although it is sometimes used.

## 6. Conclusions

The new expression for  $\beta$  (eq 19) asserts, in fact, that only the second moment of the transition probability is important. This new  $\beta$  is seen to perform quite well with a minimum of computational labor, once the transition matrix  $\mathbf{Q}$  is set up; in fact  $\beta$  of eq 19 performs better than  $\beta_{\text{trad}}$  of eq 34 if weak-collision data near the low-pressure limit are not required. At or near the low-pressure limit,  $\beta_{\text{trad}}$  can be obtained quickly and with reasonable accuracy using  $k_{0,\text{wc}}$  calculated from eq 24.

If short machine time is not the primary consideration, the actual  $k_{\text{uni,wc}}$  as the lowest eigenvalue of the transition matrix  $\mathbf{J}$  can be also be obtained directly from eq 24, but the calculation has to be repeated for every value of  $\omega$ . Some caution is required here since the approximation involved in eq 24 is poor if the lowest eigenvalue is not well separated from the others; in that case eq 24 can be modified<sup>26</sup> to obtain a better approximation

$$\mu_1 \approx -1 / (\text{Tr } \mathbf{M}^{-n})^{1/n} \quad (36)$$

However, for  $n$  larger than 3 or 4 not much is gained and an actual eigenvalue determination with an eigenvalue package is preferable. As an alternative to actual eigenvalue determination of  $\mathbf{J}$ , an iterative scheme proposed by Malins and Tardy<sup>27</sup> could be used.

(26) Snider, N. S. *J. Chem. Phys.* **1976**, *65*, 1800.

Analytic formulas for the stepladder model based on eq 24 are available.<sup>5c,28</sup>

The advantage of the proposed  $\beta$  is that it, and consequently also the falloff of  $k_{\text{uni,wc}}$ , can be calculated for any specified model of the transition probability, and therefore the falloff reflects the properties of that particular model (a conclusion arrived at previously in ref 1) rather than some average model-independent property, such<sup>4</sup> as  $\langle \Delta E \rangle_{\text{down}}$ . This is of some importance since the data in Table I suggest that  $\beta$  may be different for different models, even if they have similar  $\langle \Delta E \rangle_{\text{down}}$ . Conversely, curves E1 and SL1 in Figure 2 show that almost identical  $\langle \Delta E \rangle$ 's can give rise to different  $\langle \Delta E \rangle_{\text{down}}$ 's. The practical disadvantage, of course, is that the model of the transition probability model is not known for a specific collider system.

The reasonable success of eq 20 with a constant  $\beta$  to account for the falloff of  $k_{\text{uni}}$ , as shown in Figure 3, suggests that the *shape* (or curvature) of the falloff curve is only very weakly dependent on the transition probability model and is in fact quite close to the strong-collision shape.

Finally, there are limitations of the matrix approach itself. One is related to finite matrix size, i.e., "graining", meaning that too coarse a discretization of the energy space can cause errors unless precautions are taken. The other is that round-off errors accumulate with each matrix operation. This second source of errors is minimized in the present approach by limiting the number of operations; it can, however, play a role if  $k_{\text{uni,wc}}$  is numerically very large or very small.

(27) Malins, R. J.; Tardy, D. C. *Chem. Phys. Lett.* **1978**, *57*, 289.

(28) Pritchard, H. O.; Vatsya, S. R. *Can. J. Chem.* **1984**, *62*, 1867.

## Periodic Trends in Chemical Reactivity: Reactions of $\text{Sc}^+$ , $\text{Y}^+$ , $\text{La}^+$ , and $\text{Lu}^+$ with $\text{H}_2$ , $\text{D}_2$ , and HD

J. L. Elkind, L. S. Sunderlin,

*Department of Chemistry, University of California, Berkeley, California 94720*

and P. B. Armentrout\*,†

*Department of Chemistry, University of Utah, Salt Lake City, Utah 84112 (Received: July 28, 1988; In Final Form: November 1, 1988)*

The reactions of  $\text{Sc}^+$ ,  $\text{Y}^+$ ,  $\text{La}^+$ , and  $\text{Lu}^+$  with  $\text{H}_2$ ,  $\text{D}_2$ , and HD are examined by use of guided ion beam mass spectrometry.  $\text{Sc}^+$ ,  $\text{Y}^+$ , and  $\text{La}^+$  are found to react primarily via an insertion mechanism, while  $\text{Lu}^+$  reacts impulsively at threshold and in a direct manner at higher energies. A simple molecular orbital model coupled with adiabatic surface crossings is used to explain the reactivity seen. The results are analyzed to give the 0 K bond energies  $D^\circ(\text{Sc}^+-\text{H}) = 2.44 \pm 0.09$  eV,  $D^\circ(\text{Y}^+-\text{H}) = 2.66 \pm 0.06$  eV,  $D^\circ(\text{La}^+-\text{H}) = 2.48 \pm 0.09$  eV, and a more tentative value of  $D^\circ(\text{Lu}^+-\text{H}) = 2.11 \pm 0.16$  eV (48.6  $\pm$  3.7 kcal/mol). The results suggest that intrinsic  $\text{M}^+-\text{H}$  bond dissociation energies for third-row metals are about 60 kcal/mol, similar to values for the first and second rows.

### Introduction

Over the past few years, our studies of the kinetic energy dependence of reactions of atomic transition-metal ions with  $\text{H}_2$  to form  $\text{MH}^+$  have been aimed at a comprehensive description of the effect of 4s and 3d orbital populations on reactivity.<sup>1</sup> To this end, we have altered the electron configuration of the metal ion in two ways: by moving smoothly *across* the periodic table and by producing various populations of ground and excited states

through several ion production techniques. The present report completes this work for the first-row transition metals by describing the reactions of atomic scandium ions with  $\text{H}_2$ . Further, we extend the scope of this research *down* the periodic table by describing the reactions of  $\text{H}_2$  with scandium's isovalent analogues: yttrium, lanthanum, and lutetium. This comparison allows us to test whether our description of how electron configuration dictates the interactions of atomic first-row transition-metal ions with  $\text{H}_2$

\*NSF Presidential Young Investigator, 1984-1989; Alfred P. Sloan Fellow; Camille and Henry Dreyfus Teacher-Scholar, 1988-1993.

(1) Elkind, J. L.; Armentrout, P. B. *J. Phys. Chem.* **1987**, *91*, 2037-2045, and references therein.

still holds for the heavier metals. An article discussing the reaction of these same metal ions with  $\text{CH}_4$  and  $\text{C}_2\text{H}_6$  will be published soon.<sup>2</sup>

Our previous work has identified three specific ways in which a transition-metal ion tends to interact with dihydrogen and the electronic environments associated with each type of interaction.<sup>1</sup> The relationship between these can be understood by using molecular orbital (MO) arguments. These are briefly outlined as follows. (1) *Insertion*. If the 4s and 3d $\sigma$  orbitals are unoccupied, the  $\text{M}^+ + \text{H}_2$  system reacts efficiently. The branching ratio in reaction with HD is nearly 1:1. Overall the behavior is nearly statistical. MO concepts indicate that electronic states of this type should be able to insert into  $\text{H}_2$  to form a metal dihydride intermediate (although not necessarily the ground-state  $\text{MH}_2^+$  species). (2) *Direct reaction*. If either the 4s or the 3d $\sigma$  orbital is half-occupied, the system can react efficiently via a direct mechanism if the metal ion has low spin (the same spin as ground-state  $\text{MH}_2^+$ ). The branching ratio in reaction with HD is 3–4:1 in favor of the  $\text{MH}^+$  product. MO concepts indicate that these states prefer a collinear geometry but that other geometries are not unfavorable. (3) *Impulsive reaction*. If either the 4s or 3d $\sigma$  orbital is occupied and the ion has high spin, the system reacts inefficiently at the thermodynamic threshold and via an impulsive, pairwise mechanism at elevated energies. The branching ratio in reaction with HD favors production of the  $\text{MD}^+$  product at low energies. MO concepts indicate that these states should have repulsive potential energy surfaces that strongly favor a collinear collision. The thresholds for reaction and the peaks in the cross sections tend to be delayed.

The predictive utility of this reasonably simple set of regulations is obvious and well documented. Investigations that extend these rules to larger organometallic systems have already begun to appear in the literature.<sup>2–6</sup> However, it is important to note that these ideas hold for *adiabatic* interactions, i.e., where the atomic orbital populations remain constant throughout the reaction. The predictions can fail if *adiabatic* interactions occur, i.e., the diabatic surfaces undergo avoided crossings to form adiabatic surfaces. For reactions of metal ions with dihydrogen, the reaction of  $\text{Ti}^+$  with  $\text{H}_2$  is the only one for which adiabatic behavior has been (and has needed to be) postulated,<sup>7</sup> although such behavior is quite evident in the exothermic reactions of  $\text{Fe}^+$  with large alkanes.<sup>5</sup> As we shall see, such behavior is also required to understand the systems under investigation here.

### Potential Energy Surfaces

Before discussing our experimental results, it is useful to consider the gross features of the potential energy surfaces for reaction of  $\text{M}^+$  with  $\text{H}_2$  to form  $\text{MH}^+ + \text{H}$ . In the present case, this is aided by the ab initio calculations of Rappe and Upton on the interaction of  $\text{Sc}^+$  with  $\text{H}_2$ .<sup>8</sup> This provides the first opportunity to see whether the qualitative molecular orbital arguments we have used previously<sup>1</sup> can be verified by more exacting theoretical treatments.

We should note that these four fairly similar divalent metal ions have some commanding differences in the ordering of their electronic states and their relative spacings (Table I). For instance, the  $\text{Sc}^+$  and  $\text{Y}^+$  ions used in this experiment are primarily in  $a^3\text{D}(\text{sd})$  states, while the  $\text{La}^+$  ions are primarily  $a^3\text{F}(\text{d}^2)$ , and the  $\text{Lu}^+$  ions are almost all  $1^1\text{S}(\text{s}^2)$ . Thus, we need to consider the  $a^3\text{D}(\text{sd})$ ,  $a^3\text{F}(\text{d}^2)$ , and  $1^1\text{S}(\text{s}^2)$  states of  $\text{M}^+$  and also the low-lying  $a^1\text{D}(\text{sd})$  and  $b^1\text{D}(\text{d}^2)$  states. Only  $\text{H}_2(1^1\Sigma_g^+)$  and  $\text{H}(2^1\text{S})$  need to be considered. In the following discussion, we detail only the  $\text{Sc}^+ + \text{H}_2$  system. The other systems are discussed later.

TABLE I: Low-Lying Electronic States of  $\text{Sc}^+$ ,  $\text{Y}^+$ ,  $\text{La}^+$ , and  $\text{Lu}^+$

| ion           | state            | confign         | $E,^a$ eV    | population, <sup>b</sup> % |
|---------------|------------------|-----------------|--------------|----------------------------|
| $\text{Sc}^+$ | $^3\text{D}$     | 4s3d            | 0.013        | 88.6                       |
|               | $^1\text{D}$     | 4s3d            | 0.315        | 6.0                        |
|               | $^3\text{F}$     | 3d <sup>2</sup> | 0.609        | 5.4                        |
|               | $\geq^1\text{D}$ | 3d <sup>2</sup> | $\geq 1.357$ | <0.1                       |
| $\text{Y}^+$  | $^1\text{S}$     | 5s <sup>2</sup> | 0.000        | 11.6                       |
|               | $^3\text{D}$     | 5s4d            | 0.148        | 80.7                       |
|               | $^1\text{D}$     | 5s4d            | 0.409        | 6.7                        |
|               | $^3\text{F}$     | 4d <sup>2</sup> | 1.045        | 1.0                        |
|               | $\geq^3\text{P}$ | 4d <sup>2</sup> | $\geq 1.742$ | <0.1                       |
| $\text{La}^+$ | $^3\text{F}$     | 5d <sup>2</sup> | 0.147        | 69.3                       |
|               | $^1\text{D}$     | 6s5d            | 0.173        | 12.6                       |
|               | $^3\text{D}$     | 6s5d            | 0.342        | 16.4                       |
|               | $^3\text{P}$     | 5d <sup>2</sup> | 0.738        | 1.2                        |
|               | $\geq^1\text{S}$ | 6s <sup>2</sup> | $\geq 0.917$ | <0.6                       |
| $\text{Lu}^+$ | $^1\text{S}$     | 6s <sup>2</sup> | 0.000        | 99.7                       |
|               | $^3\text{D}$     | 6s5d            | 1.628        | 0.3                        |
|               | $\geq^1\text{D}$ | 6s5d            | $\geq 2.149$ | <0.01                      |

<sup>a</sup>Statistical average of all  $J$  levels. Energies taken from: Sugar, J.; Corliss, C. *J. Phys. Chem. Ref. Data* **1985**, *14*, Suppl. 2. Moore, C. E. *Natl. Stand. Ref. Data Sys., Natl. Bur. Stand.* **1971**, *35*, Vol. II. Martin, W. C.; Zalubas, R.; Hagen, L. *Natl. Stand. Ref. Data Sys., Natl. Bur. Stand.* **1978**, *60*, 1. <sup>b</sup>Maxwell-Boltzmann distribution at 2200 K.

For the product ions, ab initio calculations<sup>8–10</sup> predict that the ground state of  $\text{ScH}^+$  is  $^2\Delta$ . This state has a covalent metal–hydrogen  $\sigma$  bond,  $\sigma_b$ , which is largely 4s–1s in character. The nonbonding electron resides in the 3d $\delta$  orbital on Sc. There are also two low-lying excited states of  $\text{ScH}^+$  which differ only in the 3d orbital occupation. These are a  $^2\Pi$  state corresponding to  $\sigma_b^2(3d\pi)$  and a  $^2\Sigma^+$  corresponding to  $\sigma_b^2(3d\sigma)$ . These are calculated to lie 0.22 eV and  $0.28 \pm 0.07$  eV above the ground state.<sup>8–10</sup> In the  $^2\Delta$  and  $^2\Pi$  states, there is a significant component of 3d $\sigma$ –1s orbital interaction in the bonding as well. The  $^2\Sigma^+$  state cannot utilize this type of bonding interaction since the 3d $\sigma$  orbital is occupied by a nonbonding electron.

As the ground-state  $\text{Sc}^+(a^3\text{D}) + \text{H}_2(1^1\Sigma_g^+)$  reactants come together, they split into five triplet surfaces, some of which are degenerate depending on the symmetry of the collision. These five surfaces correlate adiabatically with the five product states,  $\text{ScH}^+(^2\Delta, ^2\Pi, ^2\Sigma^+) + \text{H}(2^1\text{S})$ . Viewing the reaction in reverse, note that this is a high spin coupling of the products (i.e., no bonding interaction) that might be expected to be somewhat repulsive. For the  $\text{Sc}^+(a^1\text{D}) + \text{H}_2(1^1\Sigma_g^+)$  reactants, they split into five potential energy surfaces (some degenerate) having singlet spin. These should also correlate adiabatically with the five product states, only now the products are low spin coupled; i.e., a favorable bonding interaction can occur. More highly excited states of the metal ion must correlate adiabatically with more highly excited products.

A more detailed view of the potential energy surfaces can be obtained by examination of simple molecular orbital (MO) ideas that we formulated for use in our previous studies.<sup>1</sup> As a metal ion approaches  $\text{H}_2$ , the outermost atomic orbital on the metal, the 4s, begins to interact with the filled  $\sigma_g(\text{H}_2)$  MO. If the approach is along the  $C_{2v}$  axis, bonding and antibonding MOs of  $a_1$  symmetry are formed. The fully occupied  $\sigma_g(\text{H}_2)$  orbital correlates with the bonding orbital, and the 4s(M) orbital diabolically correlates with the antibonding orbital. If the 4s is occupied, this results in a repulsive interaction, which can be relieved by an approach along the  $C_{\infty v}$  axis since the 4s(M) orbital now can interact with the unoccupied  $\sigma_u(\text{H}_2)$  orbital. Much like the  $\text{H} + \text{H}_2$  reaction, the 4s(M) orbital now correlates with a largely nonbonding orbital having a node in the middle of the  $\text{M}^+ - \text{H} - \text{H}$  intermediate and eventually to a 1s electron on the H-atom product.

(9) Schilling, J. B.; Goddard, W. A.; Beauchamp, J. L. *J. Phys. Chem.* **1987**, *91*, 5616–5623.

(10) Pettersson, L. G. M.; Bauschlicher, C. W.; Langhoff, S. R.; Partridge, H. *J. Chem. Phys.* **1987**, *87*, 481–492.

(2) Sunderlin, L. S.; Armentrout, P. B. *J. Am. Chem. Soc.* In press.

(3) Aristov, N.; Armentrout, P. B. *J. Phys. Chem.* **1987**, *91*, 6178–6188.

(4) Georgiadis, R.; Armentrout, P. B. *J. Phys. Chem.* **1988**, *92*, 7067.

(5) Schultz, R. H.; Elkind, J. L.; Armentrout, P. B. *J. Am. Chem. Soc.* **1988**, *110*, 411–423.

(6) Sunderlin, L. S.; Armentrout, P. B. *J. Phys. Chem.* **1988**, *92*, 1209–1219.

(7) Elkind, J. L.; Armentrout, P. B. *Int. J. Mass Spectrom. Ion Processes* **1988**, *83*, 259–284.

(8) Rappe, A. K.; Upton, T. H. *J. Chem. Phys.* **1986**, *85*, 4400–4410.

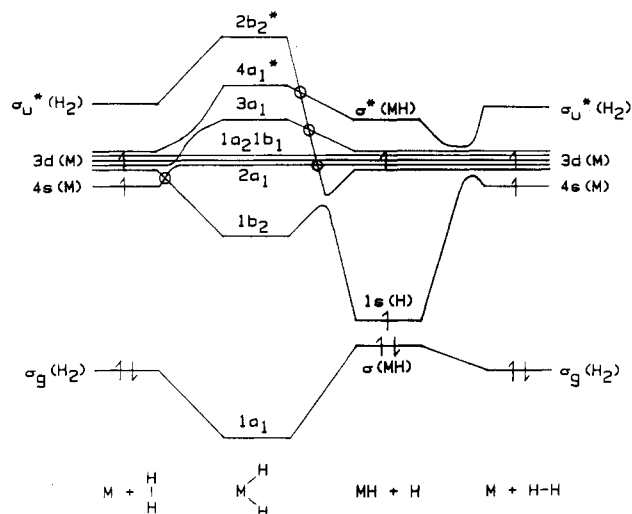


**Figure 1.** Qualitative molecular orbital correlation diagram for the interaction of a metal with  $H_2$  in  $C_{2v}$  symmetry (left side) and  $C_{nv}$  symmetry (right side). Electron occupations are indicated for  $Sc^+(sd) + H_2$  and for ground-state products,  $ScH^+ + H$ . The circles show crossings which become avoided in  $C_v$  symmetry.

If the 4s is unoccupied, the metal can approach more closely and the progress of the reaction depends on the particular 3d(M) orbitals occupied. Ideally, the 3d $\sigma$  is unoccupied since this also has repulsive interactions with the  $\sigma_g(H_2)$  orbital. In addition, it is favorable to occupy the in-plane 3d $\pi$  orbital in  $C_{2v}$  symmetry since this interacts with the unoccupied  $\sigma_u(H_2)$  MO to form bonding and antibonding MOs of  $b_2$  symmetry. This leads to formation of a dihydride intermediate that may then behave statistically. Note that this intermediate is the ground state only if the  $1b_2$  bonding orbital is doubly occupied, in which case the  $ScH_2^+$  is in a singlet state.

These diabatic correlations are shown for the case of  $Sc^+$  in Figure 1. This diagram is similar to that for other first-row metal ions<sup>1</sup> with one significant difference: the energy of the 4s orbital of  $Sc^+$  is below that of the 3d orbitals. For most metal ions, the 4s orbital diabatically and adiabatically correlates with the strongly antibonding  $4a_1^*$  MO. This orbital is the primary controlling factor in the reactivity of these ions and leads to the "rules" outlined in the Introduction. However, for  $Sc^+$ , the 4s correlates adiabatically with the nonbonding  $2a_1(3d\delta)$  orbital in  $C_{2v}$  symmetry. If  $C_{2v}$  symmetry is broken (the case in most collisions), the situation is even more favorable since in  $C_v$  symmetry (where the  $a_1$  and  $b_2$  orbitals are both  $a'$ ), the 4s orbital adiabatically correlates to the bonding  $1b_2$  orbital. These orbital interactions make it clear that  $Sc^+$  is not expected to behave diabatically.

Referring now to the behavior of specific states of the metal ion,  $Sc^+(a^3D, sd)$  and  $Sc^+(a^1D, sd)$  should prefer to react diabatically via a collinear geometry due to the occupation of the 4s orbital.  $Sc^+(1S, s^2)$  should be very repulsive and react impulsively. In contrast, the diabatic behavior of  $Sc^+(a^3F, d^2)$  and  $Sc^+(b^1D, d^2)$  should be insertion for most configurations, since these states avoid the repulsive interaction between the 4s orbital and the  $H_2(\sigma_g)$  in  $C_{2v}$  symmetry. Adiabatically, surfaces evolving from  $Sc^+(a^3D)$  and  $Sc^+(a^3F)$  cross one another (corresponding to the crossing between the 4s and 3d orbitals), as do the surfaces evolving from  $Sc^+(a^1D)$  and  $Sc^+(b^1D)$ . Thus, the reactivity of  $Sc^+(a^3D)$  and  $Sc^+(a^1D)$  may resemble that of a  $d^2$  configuration.

These ideas are in good agreement with the theoretical study of Rappe and Upton.<sup>8</sup> They conclude that both the  $a^3D(sd)$  ground and  $a^1D(sd)$  first excited states are likely to react with  $H_2$  to form  $ScH^+$ . Reaction will be most efficient in a collinear interaction geometry, but other interaction angles are probably reactive as well. These calculations also show that the reactive surfaces entail considerable adiabatic interactions between surfaces evolving from states having the same spin. In particular, the perpendicular approaches clearly show avoided crossings between three of the surfaces evolving from the  $a^3D(sd)$  state with those of the  $a^3F(d^2)$  state, and between four of the surfaces evolving

from the  $a^1D(sd)$  state with those of the  $b^1D(d^2)$  state. One of these singlet surfaces leads to formation of ground-state  $ScH_2^+(^1A_1)$ . The  $1b_2$  MO of the  $ScH_2^+$  intermediate is occupied for all surfaces involved in the crossings.

Rappe and Upton also considered whether there was any interaction between the triplet and singlet surfaces via spin-orbit coupling. Their calculations suggest that, for the case of scandium, such coupling is weak. While the extent of such coupling is difficult to predict, we expect that this effect may be more important for the heavier ions since they have larger atomic spin-orbit interactions.

## Experimental Section

**General.** A complete description of the apparatus and experimental procedures is given elsewhere.<sup>11</sup> Briefly, the apparatus comprises three differentially pumped vacuum chambers. In the first chamber, ions are produced as described below. The resulting ions are extracted, accelerated, and focused into a magnetic sector momentum analyzer for mass analysis. In the second vacuum chamber, the mass-selected ions are decelerated to a desired kinetic energy and focused into an octopole ion guide. Radio frequency electric fields in the guide create a radial potential well that traps ions over the mass range studied. The velocity of the ions parallel to the axis of the guide is unchanged. The octopole passes through a static gas cell into which the reactant gas can be introduced. Pressures, which are measured by a MKS Baratron capacitance manometer, are maintained at a sufficiently low level (less than 1.0 mTorr) that multiple ion-molecule collisions are improbable. The octopole ion guide ensures efficient collection of all ionic products and transmitted reactant ions. Product ion losses due to dynamic effects are small.<sup>11</sup> High product collection gives better sensitivity, allowing cross sections as small as  $10^{-19}$  cm<sup>2</sup> to be measured. Thus, use of the octopole provides much better precision in the crucial threshold region of endothermic reactions, as well as the ability to accurately monitor minor products. The ions are extracted from the octopole and focused into the third vacuum chamber, which contains a quadrupole mass filter for product mass analysis. Ions are detected with a secondary electron scintillation ion detector and processed by pulse-counting techniques. The experiments are automated by use of a DEC MINC computer, which collects the ion signals at different masses as it increments the incident ion energy.

A major experimental advantage of an octopole ion guide is that the absolute energy of the ions in the interaction region can be measured easily by using the octopole as a retarding field analyzer. Because the retarding region is physically the same as the interaction region, this energy measurement has minimal uncertainties due to space charge, contact potentials, and focusing aberrations. By scanning through the nominal ion energy zero (where the dc potential on the octopole equals the potential in the ion source), an ion intensity cutoff curve is obtained. The differential of this curve is represented well by a Gaussian peak. The center of this peak is taken to be the true zero of the ion energy, and its width characterizes the kinetic energy distribution of the ion beam. The fwhm of the energy distribution is independent of energy and is typically  $\approx 0.7$  eV lab. Uncertainties in the absolute energy scale are  $\pm 0.05$  eV lab. The behavior of the octopole as a retarding analyzer has been verified by time-of-flight measurements<sup>11</sup> and comparisons with theory.<sup>11,12</sup>

Translational energies in the laboratory frame of reference are related to energies in the center of mass (CM) frame by  $E(CM) = E(lab)m/(M + m)$ , where  $M$  and  $m$  are the masses of the incident ion and neutral reactant, respectively. The <sup>45</sup>Sc isotope (100% natural abundance), <sup>89</sup>Y isotope (100% natural abundance), <sup>139</sup>La isotope (99.9% natural abundance), and <sup>175</sup>Lu isotope (97.4% natural abundance) were used in these experiments. Below  $\sim 0.3$  eV lab, the energies are corrected for truncation of the ion beam

(11) Ervin, K. M.; Armentrout, P. B. *J. Chem. Phys.* **1985**, *83*, 166-189.

(12) Ervin, K. M.; Armentrout, P. B. *J. Chem. Phys.* **1986**, *84*, 6738-6749, 6750-6760. Burley, J. D.; Ervin, K. M.; Armentrout, P. B. *Int. J. Mass Spectrom. Ion Processes* **1987**, *80*, 153-175.

energy distribution as described previously.<sup>11</sup> The data obtained in this experiment are broadened by two effects: the ion energy spread and thermal motion of the neutral gas (Doppler broadening).<sup>13</sup> The ion energy spread has a width in the CM frame of  $<0.06$  eV. The second effect has a width (in eV) in the CM frame of  $\sim 0.053E^{1/2}$  for the reactions of  $\text{Sc}^+$ ,  $\text{Y}^+$ ,  $\text{La}^+$ , and  $\text{Lu}^+$  with  $\text{H}_2$ ,  $\text{HD}$ , and  $\text{D}_2$ .<sup>13</sup> The resultant energy distribution effectively broadens any sharp features in the excitation function. When model cross sections are compared to experimental data, the calculated cross sections are convoluted with both sources of experimental energy broadening.<sup>11</sup>

Raw ion intensities are converted to absolute cross sections as described previously.<sup>11</sup> The accuracy of our absolute cross sections is estimated to be  $\pm 20\%$ . Uncertainties at low cross section values are generally about  $\pm 10^{-19}$  cm<sup>2</sup>, primarily because of random counting noise (typically  $\leq 10$  counts/s). Uncertainties are somewhat higher for hydride channels because of overlap in the mass spectrometer with the intense neighboring  $\text{M}^+$  peak.

**Ion Sources.** In this experiment, ions are produced in a surface ionization (SI) source. Here,  $\text{MCl}_3$  (where  $\text{M} = \text{Sc}, \text{Y}, \text{La},$  or  $\text{Lu}$ ) is vaporized in a resistively heated oven and directed at a rhenium filament that is resistively heated to a temperature of  $2200 \pm 100$  K, as measured by optical pyrometry. It is generally assumed that a Maxwell-Boltzmann distribution accurately describes the populations of the electronic states of the ions. Table I gives these populations for the ions at 2200 K. Since all transitions between states in Table I are parity forbidden, the radiative lifetimes of the excited states (on the order of seconds long)<sup>14</sup> are expected to be much greater than the flight time between the ionization and reaction regions ( $\sim 10$ – $100$   $\mu\text{s}$ ). Thus, very few excited ions radiatively relax before reaction.

The assumption that the populations of electronic states of ions emitted from an SI source are given by a Maxwell-Boltzmann distribution at the filament temperature is important. Unfortunately, to our knowledge the experimental population distributions of ions produced by SI have not been directly measured in any system. However, many experiments support the characterization of SI as a thermal process, as discussed previously.<sup>6</sup> In the specific case of transition-metal ions, the Maxwell-Boltzmann population assumption has been verified indirectly by comparing experimental cross section magnitudes for specific metal ion states to those calculated by phase space theory, those measured using an electron impact (EI) source, and those measured using a drift cell source that produces ground-state ions exclusively.<sup>3,5-7,15</sup> The relative magnitude of cross sections for ions created at different filament temperatures has also been found to be consistent with a Maxwell-Boltzmann distribution.<sup>3,6</sup> A more direct test is provided by comparison of surface ionization data<sup>16</sup> to recent measurements of Weisshaar and co-workers who produced vanadium ions with known state distributions by using resonant multiphoton ionization.<sup>17</sup> While not utterly conclusive, the data for a wide variety of transition-metal ions suggest that a Maxwell-Boltzmann distribution of electronic states is created by SI.

In previous studies, reactant ion state populations were varied by using the more vigorous ionization method of EI and, in some cases, by relaxing the beam to pure ground state in a high-pressure drift cell. Neither of these methods can be used in this study since we have found no suitably volatile yet thermally stable compounds of scandium, yttrium, lanthanum, or lutetium that produce atomic transition-metal ions without impurities of the same mass during EI ionization.

The metal chlorides are obtained from Aesar and are used without further purification. HD has been prepared by standard

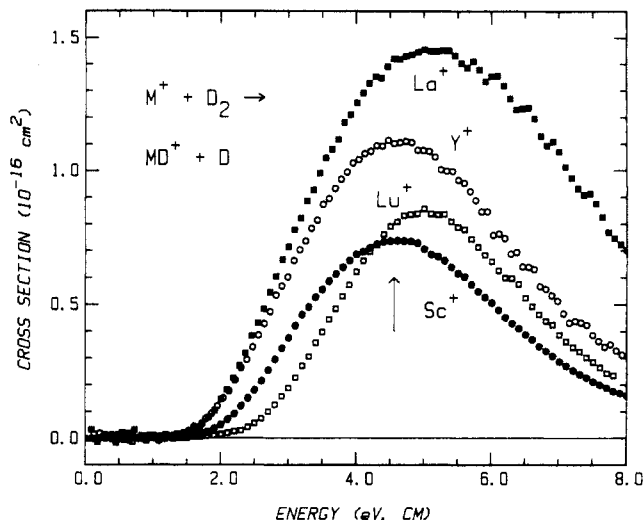


**Figure 2.** Cross sections for the reactions of  $\text{Sc}^+$  (closed circles),  $\text{Y}^+$  (open circles),  $\text{La}^+$  (closed squares), and  $\text{Lu}^+$  (open squares) with  $\text{D}_2$  as a function of kinetic energy in the center of mass frame. The arrow indicates the bond dissociation energy of  $\text{D}_2$  at 4.56 eV.

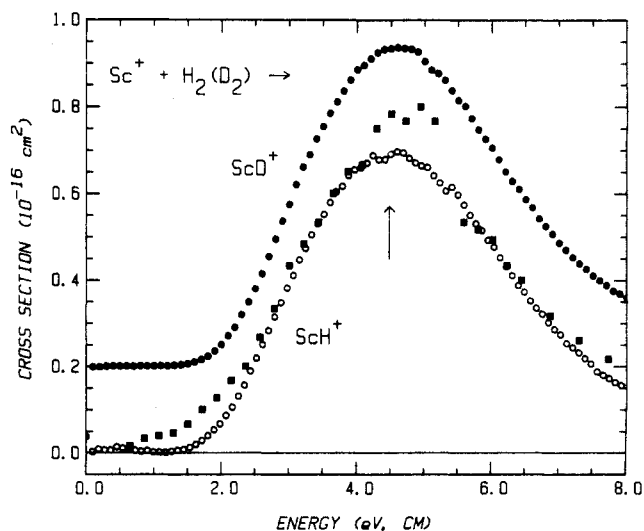
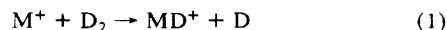


**Figure 3.** Cross sections for the reaction of  $\text{Sc}^+$  with  $\text{H}_2$  (open circles) and  $\text{D}_2$  (closed circles, zero offset by  $0.2 \text{ \AA}^2$ ) as a function of kinetic energy in the center of mass frame. The solid squares show data from ref 19 scaled down by a factor of 3. The arrow indicates the bond dissociation energy of  $\text{H}_2$  at 4.48 eV.

procedures.<sup>18</sup> Purity of  $>96\%$  HD was confirmed by mass spectrometric analysis. Impurities are primarily  $\text{H}_2$  and  $\text{D}_2$  in nearly equal amounts as confirmed by Raman spectroscopic analysis.

## Results

**Reactions with  $\text{H}_2$  and  $\text{D}_2$ .** Figure 2 shows the experimental excitation functions for reaction 1



where  $\text{M} = \text{Sc}, \text{Y}, \text{La},$  and  $\text{Lu}$ . In all cases, the metal ions are produced by surface ionization (SI). The general shapes of the cross sections are quite typical for endothermic reactions. In each case, the cross section rises from an apparent threshold at 1.5–2 eV, reaches a maximum near 4.5 eV, and then declines at higher energies. The peaks are near the bond dissociation energy of  $\text{D}_2$ , 4.56 eV. The maximum magnitudes of the cross sections for  $\text{Y}$ ,  $\text{La}$ , and  $\text{Lu}$  are larger than that for  $\text{Sc}$  by 50%, 100%, and 15%, respectively. The apparent thresholds and shapes of the cross

(13) Chantry, P. J. *J. Chem. Phys.* **1971**, *55*, 2746–2759.

(14) Garstang, R. H. *Mon. Not. R. Astron. Soc.* **1962**, *124*, 321; private communication.

(15) Elkind, J. L.; Armentrout, P. B. *J. Phys. Chem.* **1985**, *89*, 5626–5636; *Ibid.* **1986**, *90*, 5736–5745, 6576–6586; *Ibid.* **1987**, *91*, 2037–2045; *J. Chem. Phys.* **1986**, *84*, 4862–4871; *Ibid.* **1987**, *86*, 1868–1877.

(16) Aristov, N.; Armentrout, P. B. *J. Am. Chem. Soc.* **1986**, *108*, 1806–1819.

(17) Sanders, L.; Hanton, S.; Weisshaar, J. C. *J. Phys. Chem.* **1987**, *91*, 5145–5148.

(18) Wender, I.; Friedel, R. A.; Orchin, M. *J. Am. Chem. Soc.* **1949**, *71*, 1140.

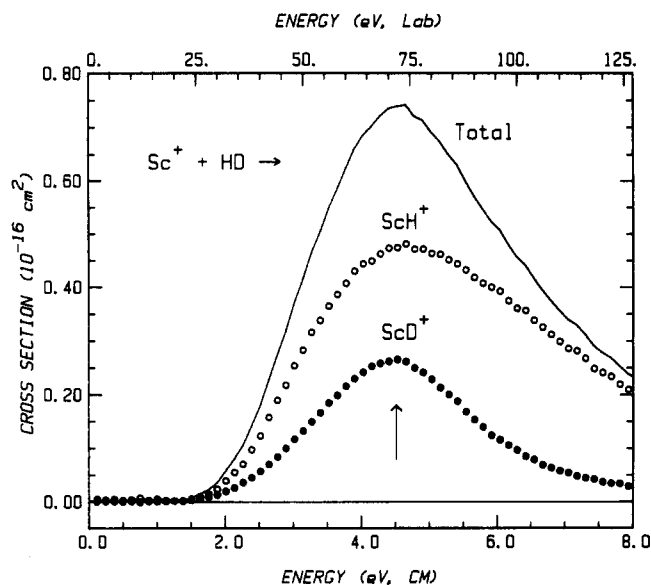


**Figure 4.** Cross sections for the reaction of  $\text{Sc}^+$  with HD as a function of kinetic energy in the center of mass frame (lower scale) and laboratory frame (upper scale). Open and closed circles show the results for production of  $\text{ScH}^+$  and  $\text{ScD}^+$ , respectively. The line shows the total cross section. The arrow indicates the bond dissociation energy of HD at 4.52 eV.

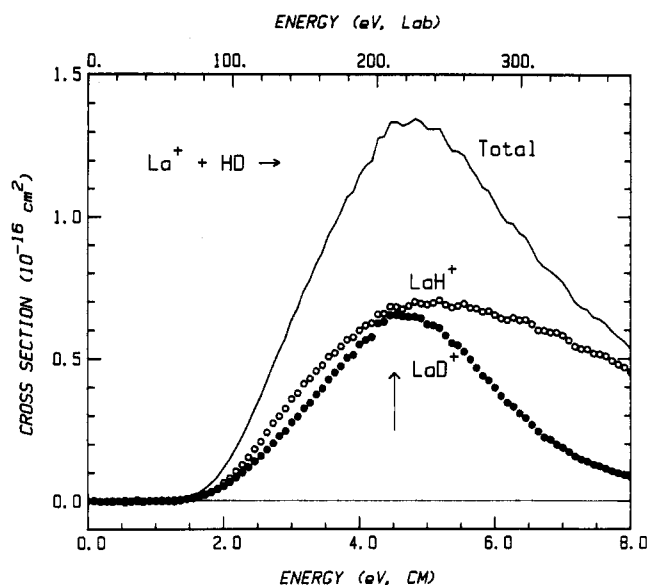


**Figure 6.** Cross sections for the reaction of  $\text{La}^+$  with HD as a function of kinetic energy in the center of mass frame (lower scale) and laboratory frame (upper scale). Open and closed circles show the results for production of  $\text{LaH}^+$  and  $\text{LaD}^+$ , respectively. The line shows the total cross section. The arrow indicates the bond dissociation energy of HD at 4.52 eV.

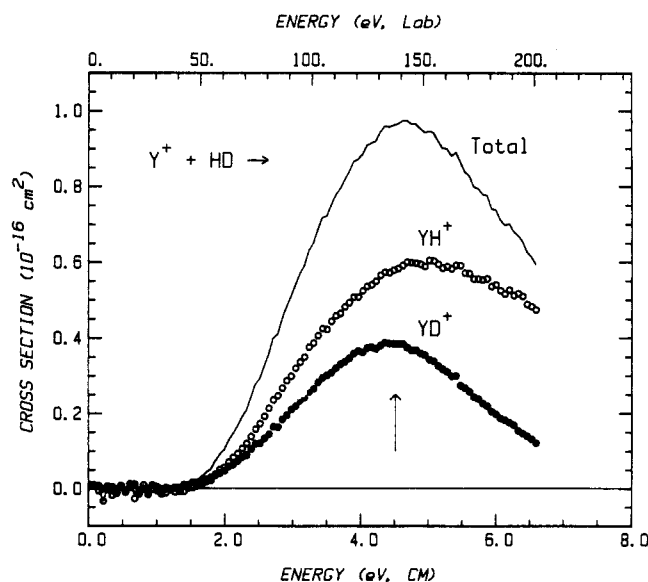


**Figure 5.** Cross sections for the reaction of  $\text{Y}^+$  with HD as a function of kinetic energy in the center of mass frame (lower scale) and laboratory frame (upper scale). Open and closed circles show the results for production of  $\text{YH}^+$  and  $\text{YD}^+$ , respectively. The line shows the total cross section. The arrow indicates the bond dissociation energy of HD at 4.52 eV.

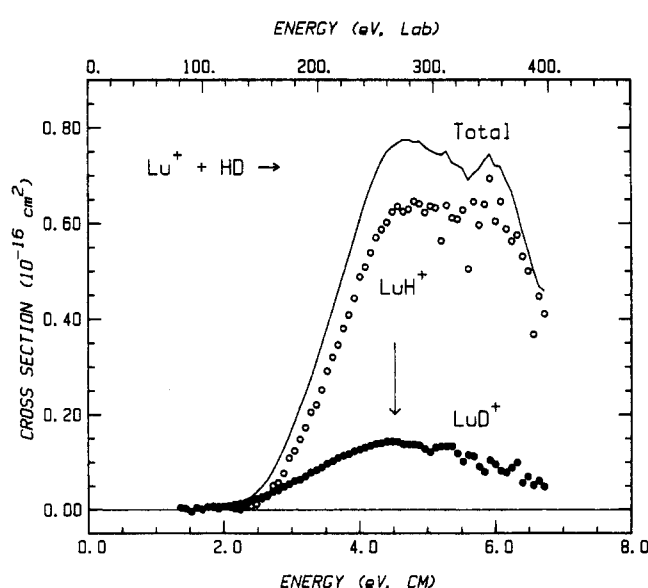
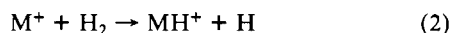


**Figure 7.** Cross sections for the reaction of  $\text{Lu}^+$  with HD as a function of kinetic energy in the center of mass frame (lower scale) and laboratory frame (upper scale). Open and closed circles show the results for production of  $\text{LuH}^+$  and  $\text{LuD}^+$ , respectively. The line shows the total cross section. The arrow indicates the bond dissociation energy of HD at 4.52 eV.

sections in the threshold region are very similar for Sc, Y, and La. For Lu, the onset of reactivity is slower than for the other ions (Figure 2). Indeed, the shape of the cross section is similar but shifted up in energy by  $\approx 0.6$  eV. At high energies ( $>4.5$  eV), the declines in the cross sections are similar for Sc and Y, but those for La and Lu are delayed by  $\approx 1$  eV.

Results for reaction 2



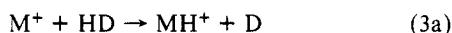
were also obtained for  $\text{M} = \text{Sc}$  and  $\text{Y}$ . In both cases, the cross sections are similar in shape to the  $\text{D}_2$  results, as shown in Figure 3 for the case of Sc. However, they have slightly different magnitudes:  $\approx 5\%$  smaller for Sc and  $10\%$  larger for Y. These differences are within the experimental uncertainty. Reaction 2 where  $\text{M} = \text{Sc}$  has been studied previously by Tolbert and Beauchamp (TB).<sup>19</sup> Their results are also reproduced in Figure

3. The data are in reasonable qualitative agreement with the present data, but are  $\approx 3$  times larger.<sup>20</sup> On the basis of the similarity of the results for reactions 1 and 2 where  $\text{M} = \text{Sc}$ , or  $\text{Y}$ , we expect comparable results for  $\text{M} = \text{La}$  or  $\text{Lu}$ . Studies of reaction 2 with these heavier metals were not performed since they are not expected to yield additional insight and they are experimentally much more difficult due to mass resolution.

**Reactions with HD.** Figures 4–7 show the product excitation functions for reactions 3a and 3b

(19) Tolbert, M. A.; Beauchamp, J. L. *J. Am. Chem. Soc.* **1984**, *106*, 8117–8122.

(20) Since the cross sections are calculated from a ratio of the product intensities to reactant ion intensities, this result is believed to be due to excessive losses in the incident ion beam compared to the product ions in the apparatus used by TB, which has no octopole ion guide.



where M = Sc, Y, La, and Lu, respectively. Again the metal ions have been produced by SI. In each case, the total cross sections are similar in shape to the H<sub>2</sub> and D<sub>2</sub> cross sections, except that the La<sup>+</sup> + HD cross section peaks and falls off somewhat sooner than the D<sub>2</sub> cross section. This makes the La<sup>+</sup> + HD cross section closer in shape to the Sc<sup>+</sup> and Y<sup>+</sup> cross sections. The HD cross sections are somewhat smaller than the D<sub>2</sub> cross sections, by 0%, 15%, 10%, and 25%, respectively.

The metal ions show distinctive behavior in the branching ratios between reactions 3a and 3b. For M = Sc, Y, and La, formation of MH<sup>+</sup> is favored over formation of MD<sup>+</sup> by factors of approximately 2.0, 1.4, and 1.2, respectively. The behavior of Lu<sup>+</sup> is quite different from the other three systems. At threshold, LuD<sup>+</sup> is favored by approximately 4:1. As the energy increases, the LuH<sup>+</sup>:LuD<sup>+</sup> ratio increases monotonically, with LuH<sup>+</sup> the preferred product by roughly 4:1 at 4.5 eV.

In all four systems, both reaction channels and the total cross sections peak near 4.52 eV, the HD bond dissociation energy. Above this energy, the MH<sup>+</sup> channels fall off much more slowly than the MD<sup>+</sup> channels. This high-energy behavior is typical for reactions of atomic ions with HD. It is due to the fact that the heavier D atom can carry away more energy than an H atom, thus stabilizing MH<sup>+</sup> relative to MD<sup>+</sup>.

### Thermochemical Analysis

We can derive metal-hydride ion bond energies by measuring the energy threshold for formation of MH<sup>+</sup>,  $E_0(\text{H}_2)$ , and then converting to the bond dissociation energy of MH<sup>+</sup> at 0 K by using eq 4

$$D^{\circ}_0(\text{MH}^+) = D^{\circ}_0(\text{H}_2) - E_0(\text{H}_2) \quad (4)$$

and the value  $D^{\circ}_0(\text{H}_2) = 4.478$  eV. This equation assumes that no barrier to reaction in excess of the endothermicity exists. This is an assumption that is generally valid for ion-molecule reactions and one that we have tested previously.<sup>21,22</sup>

For the reactions covered in the present report, the greatest uncertainty in deriving  $E_0(\text{H}_2)$ , the threshold for producing ground-state products from ground state reactants, comes from a lack of quantitative knowledge of the relative reactivity of the different states populated in the SI beam. For several other systems, we were able to observe the reaction of a single state and this simplified the thermochemical analysis. For the Sc<sup>+</sup>, Y<sup>+</sup>, and La<sup>+</sup> systems, several states are always present and presumed reacting. In the absence of experimental information to the contrary, we assume all states are present with populations given by Table I and that they have equal reactivity. This is our standard procedure for cases such as these.<sup>1</sup> In the case of Lu<sup>+</sup>, it is assumed that the only state that reacts is the ground state, since the only significantly populated excited state is expected to react inefficiently, as discussed below.

**Threshold Behavior.** The threshold behavior of endothermic reactions has been discussed previously.<sup>7,15,16,23</sup> In the present cases where several ion states (denoted by *i*) are involved, we parameterize the cross sections in the threshold region by equation 5<sup>1,7</sup>

$$\sigma(E) = \sum_i g_i \sigma_{i0} (E - E_0 + E_{\text{rot}} + E_i)^n / E^m \quad (5)$$

where  $g_i$  is the population of the various states,  $\sigma_{i0}$  are scaling factors having units of Å<sup>2</sup> eV<sup>(m-n)</sup>,  $E$  is the relative translational energy of the reactants, and  $n$  and  $m$  are adjustable parameters.

TABLE II: Threshold Energies and Models<sup>a</sup>

| reaction                         | model <sup>b</sup> |             |             |                  |                  |
|----------------------------------|--------------------|-------------|-------------|------------------|------------------|
|                                  |                    | $m = 1$     | $n = m$     | LOC <sup>c</sup> | PST <sup>d</sup> |
| Sc <sup>+</sup> + H <sub>2</sub> | $E_0$              | 2.02 (0.11) | 1.97 (0.12) | 1.99 (0.05)      | 1.94 (0.05)      |
|                                  | $n$                | 1.3 (0.2)   | 1.6 (0.4)   |                  |                  |
| Sc <sup>+</sup> + D <sub>2</sub> | $E_0$              | 2.15 (0.03) | 2.11 (0.03) | 2.09 (0.03)      | 2.04 (0.03)      |
|                                  | $n$                | 1.3 (0.1)   | 1.6 (0.2)   |                  |                  |
| Y <sup>+</sup> + H <sub>2</sub>  | $E_0$              | 1.84 (0.10) | 1.82 (0.11) | 1.83 (0.06)      | 1.80 (0.06)      |
|                                  | $n$                | 1.6 (0.1)   | 2.2 (0.3)   |                  |                  |
| Y <sup>+</sup> + D <sub>2</sub>  | $E_0$              | 1.85 (0.03) | 1.83 (0.04) | 1.88 (0.02)      | 1.85 (0.02)      |
|                                  | $n$                | 1.6 (0.1)   | 2.2 (0.2)   |                  |                  |
| La <sup>+</sup> + D <sub>2</sub> | $E_0$              | 2.05 (0.09) | 2.04 (0.11) |                  |                  |
|                                  | $n$                | 1.4 (0.2)   | 1.8 (0.4)   |                  |                  |
| Lu <sup>+</sup> + D <sub>2</sub> | $E_0$              | 2.49 (0.12) | 2.35 (0.19) |                  |                  |
|                                  | $n$                | 1.5 (0.2)   | 2.1 (0.5)   |                  |                  |

<sup>a</sup>Uncertainties (one standard deviation) are in parentheses. <sup>b</sup>Model refers to the values of  $n$  and  $m$  in eq 5. <sup>c</sup>Line-of-centers model,  $n = m = 1.0$  in eq 5. Values are for results obtained when excited product states are considered explicitly. <sup>d</sup>Phase space theory; see text. Values are for results obtained when excited product states are considered explicitly.

Here,  $E_0$  is the threshold for reaction of the lowest  $J$  state of the ion,  $E_{\text{rot}}$  (=0.024 eV) is the average rotational energy of the reacting H<sub>2</sub> molecule, and  $E_i$  is the electronic excitation of each particular  $J$  state (for Sc<sup>+</sup> and Y<sup>+</sup>, where the splitting of  $J$  levels within an electronic state is small, the  $J$ -averaged values given in Table I are used). In this study, it is assumed that  $n$ ,  $m$ , and  $\sigma_{i0}$  in eq 5 are the same for all states (except for Lu, where only the ground state is considered, as discussed above). The reaction of M<sup>+</sup> with D<sub>2</sub> is also used to derive  $D^{\circ}_0(\text{M}^+-\text{H})$  after adjusting for zero-point-energy differences in the reactants and products.<sup>24</sup> Reactions with HD are not used in deriving thermochemistry because of difficulties in treating the branching ratios between the two products.

As in previous studies,<sup>7,15</sup> we utilize the line-of-centers (LOC) model where  $n = m = 1$  and also more general models where  $n$  is allowed to vary freely but  $m$  is constrained as  $n = m$  or  $m = 1$ . The other parameters ( $\sigma_{i0}$ ,  $n$ , and  $E_0$ ) are optimized by using a nonlinear least-squares analysis to give the best fit to the data after convoluting over the experimental energy distribution. The data can also be interpreted by using phase space theory (PST) to calculate theoretical cross sections. In the case of Sc<sup>+</sup> and Y<sup>+</sup>, the required molecular constants for the product ions ( $\omega_e \approx 1600$  cm<sup>-1</sup> for both ScH<sup>+</sup> and YH<sup>+</sup>,  $r_e(\text{ScH}^+) \approx 1.8$  Å, and  $r_e(\text{YH}^+) \approx 1.9$  Å) have been determined by ab initio calculations.<sup>8-10</sup> The calculated cross sections are similar to LOC fits. Information necessary for PST calculations about the rotational and vibrational modes of LaH<sup>+</sup> and LuH<sup>+</sup> is lacking, so values extrapolated from Sc<sup>+</sup> and Y<sup>+</sup> are used.

The results of this type of analysis are given in Table II. It is found that the LOC model and PST models fail to adequately reproduce the data for any of these systems. These failures are somewhat surprising since both LOC and PST models have generally provided reasonable means of interpreting the cross sections of first-row transition metals that do not react via an impulsive mechanism.<sup>1,7,15</sup> However, a similar result has been noted for the reaction of Ca<sup>+</sup> with H<sub>2</sub> and D<sub>2</sub>.<sup>25</sup> Interestingly, the LOC and PST models do reproduce the data if excited-state products are explicitly accounted for. This can only be verified for the Sc<sup>+</sup> and Y<sup>+</sup> cases where these excitation energies have been calculated: 0.22 eV for ScH<sup>+</sup>(<sup>2</sup>Π), 0.27 ± 0.07 eV for ScH<sup>+</sup>(<sup>2</sup>Σ), 0.37 eV for YH<sup>+</sup>(<sup>2</sup>Δ), and 0.66 eV for YH<sup>+</sup>(<sup>2</sup>Π).<sup>8-10</sup> Table II includes results for the LOC and PST models where this effect has been incorporated.

(21) Boo, B. H.; Armentrout, P. B. *J. Am. Chem. Soc.* **1987**, *109*, 3549-3559.

(22) Ervin, K. M.; Armentrout, P. B. *J. Chem. Phys.* **1987**, *86*, 2659-2673. Elkind, J. L.; Armentrout, P. B. *J. Phys. Chem.* **1984**, *88*, 5454-5456. Armentrout, P. B. In *Structure/Reactivity and Thermochemistry of Ions*; Ausloos, P., Lias, S. G., Eds.; Reidel: Dordrecht, 1987; pp 97-164.

(23) Sunderlin, L.; Aristov, N.; Armentrout, P. B. *J. Am. Chem. Soc.* **1987**, *109*, 78-89.

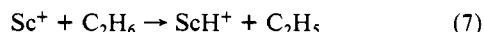
(24) In the case of D<sub>2</sub>,  $E_{\text{rot}} = 0.025$  eV and the bond energy is 4.556 eV at 0 K. Theoretical calculations give M<sup>+</sup>-H vibrational frequencies (M = Sc, Y) as about 1600 cm<sup>-1</sup>.<sup>8-10</sup> This is assumed to also hold for M = La and Lu. M<sup>+</sup>-D vibrational frequencies should therefore be about 1130 cm<sup>-1</sup>. The difference in zero-point energies can be approximated as half of the difference in the vibrational frequencies. Thus,  $D^{\circ}(\text{M}^+-\text{D})$  is stronger than  $D^{\circ}(\text{M}^+-\text{H})$  by  $\approx 235$  cm<sup>-1</sup> (0.029 eV).

(25) Georgiadis, R.; Armentrout, P. B. *J. Phys. Chem.* **1988**, *92*, 7060.

Because of the inadequacies of the LOC and PST models in the case of  $\text{La}^+$  and  $\text{Lu}^+$ , only the results obtained from the  $m = 1$  and  $m = n$  models are used in the following discussion to derive thermochemistry. The error limits cited for the bond energies are calculated from the range in the threshold values for the two sets of parameters and different data sets, and the error in the absolute energy scale. For the  $\text{Sc}^+$  and  $\text{Y}^+$  systems, the PST and LOC models provide nearly identical threshold values (Table II) when the excited product states are included in the analysis.

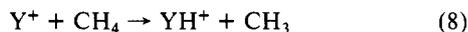
$\text{Sc}^+ + \text{H}_2$  and  $\text{D}_2$ . From the  $m = 1$  and  $n = m$  analyses shown in Table II, the threshold for reaction 2 ( $M = \text{Sc}$ ) is  $E_0 = 2.00 \pm 0.11$  eV. This gives a bond energy of  $2.48 \pm 0.11$  eV. Analysis of reaction 1 ( $M = \text{Sc}$ ) gives a threshold of  $2.13 \pm 0.04$  eV. After correcting for zero-point-energy differences, this leads to a  $\text{ScH}^+$  bond energy of  $2.40 \pm 0.04$  eV. Averaging these results gives a  $\text{ScH}^+$  bond energy of  $2.44 \pm 0.09$  eV. If the LOC and PST results of Table II are also included, the value is comparable,  $2.46 \pm 0.06$  eV. A preliminary analysis of the data presented in this paper gave  $2.40 \pm 0.10$  eV.<sup>1,26</sup> The analysis of this reaction by Tolbert and Beauchamp gave  $D^\circ(\text{Sc}^+-\text{H}) = 2.30 \pm 0.17$  eV,<sup>19</sup> within experimental error of the present result.

This bond strength has also been measured in two hydrocarbon systems. Analysis of reactions 6 and 7



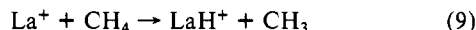
gives 0 K bond energies of  $D^\circ(\text{Sc}^+-\text{H}) = 2.48 \pm 0.06$  eV<sup>2</sup> and  $2.34 \pm 0.15$  eV,<sup>23</sup> respectively, in good agreement with the value derived here. These values are less reliable because of competing reactions and the greater number of degrees of freedom in the larger systems. Thus,  $2.44 \pm 0.09$  eV ( $56.3 \pm 2.1$  kcal/mol) is our best value for this bond energy. This value is in good agreement with *ab initio* calculations of the bond energy: 2.20,<sup>8</sup> 2.39,<sup>9</sup> 2.43,<sup>10</sup> 2.29,<sup>27</sup> and 2.37 eV.<sup>28</sup> This agreement lends credence to the means of analysis used here.

$\text{Y}^+ + \text{H}_2$  and  $\text{D}_2$ . Analysis of reactions 1 and 2 where  $M = \text{Y}$  gives an average value for  $D^\circ(\text{Y}^+-\text{H})$  of  $2.66 \pm 0.06$  eV ( $61.3 \pm 1.4$  kcal/mol). If the LOC and PST results of Table II are also included, the value is identical,  $2.66 \pm 0.05$  eV. A previous determination of this bond energy using preliminary data yielded a bond energy of  $2.52 \pm 0.13$  eV.<sup>26</sup> Analysis of reaction 8



gives a somewhat lower value of  $D^\circ(\text{Y}^+-\text{H}) = 2.26 \pm 0.15$  eV.<sup>2</sup> Theoretical values are 2.58 eV<sup>10</sup> and 2.51 eV,<sup>29</sup> again in reasonable agreement with the values derived from the  $\text{H}_2$  and  $\text{D}_2$  systems.

$\text{La}^+ + \text{D}_2$ . Analysis of reaction 1 where  $M = \text{La}$  results in a  $\text{LaH}^+$  bond energy of  $2.48 \pm 0.09$  eV ( $57.2 \pm 2.1$  kcal/mol). Analysis of reaction 9



gives  $2.36 \pm 0.23$  eV, in fair agreement with the value obtained from reaction 1. No previous measurements have been made of this bond strength, nor have calculations been done on  $\text{LaH}^+$ . We take  $2.48 \pm 0.09$  eV to be the best value for this bond strength.

$\text{Lu}^+ + \text{D}_2$ . The data for reaction 1 where  $M = \text{Lu}$  is unusual in that the cross section rises slowly at threshold and shows impulsive behavior at low energies, as indicated by the low  $\text{LuH}^+/\text{LuD}^+$  ratio in reaction 3. This makes modeling of the cross section and thus the derived thermochemistry less reliable. If the data is analyzed with no restrictions, the optimum values of  $n$  in both the  $m = 1$  and  $n = m$  models are found to be very high,

reflecting the low energy tail in the data. This analysis yields bond energies in the range of  $2.6 \pm 0.4$  eV. If this tail is ignored in the fitting analysis, results comparable to the other systems are obtained (Table II). This analysis gives a  $\text{LuH}^+$  bond energy of  $2.11 \pm 0.16$  eV ( $48.6 \pm 3.7$  kcal/mol). Because the shape of the  $\text{LuH}^+$  cross section resembles that of the other systems so closely, yet is shifted up by about 0.6 eV (Figure 2), we tend to favor this latter interpretation and report this value.

*Periodic Trends.* Previous experimental<sup>26,30</sup> and theoretical<sup>9,29</sup> work has demonstrated that the bond energies of the first-row transition-metal ions to H are correlated with the promotion energy,  $E_p$ , necessary to promote the metal ion into an electronic state suitable for bonding. In the case of group 3 elements, this electronic state is an average of the lowest singlet and triplet states with an *sd* orbital occupation. This assumes the bonding can be considered to be primarily from a singly occupied *s* orbital on the metal to the 1*s* orbital of H. *Ab initio* calculations<sup>9,10</sup> indicate that this is true for most first-row transition-metal ions. For second-row metal ions, contributions to the bonding from the 4*d* orbital are extensive. The intrinsic 0 K bond energy has been reported to be  $\approx 56$  kcal/mol for the first row and  $\approx 58$  kcal/mol for the second row of the transition metals.<sup>30</sup> Using the previously published correlations between  $D^\circ(\text{M}^+-\text{H})$  and  $E_p$  leads to estimates of 54, 56, 56, and 43 kcal/mol for the  $\text{M}^+-\text{H}$  bond energies where  $M = \text{Sc}, \text{Y}, \text{La},$  and  $\text{Lu}$ , respectively.<sup>31</sup> The experimental values are higher than predicted by  $2 \pm 2, 5 \pm 2, 1 \pm 2,$  and  $6 \pm 4$  kcal/mol. The discrepancies are not unreasonable given the semiquantitative nature of the correlation. The fact that the third-row ions match the predictions of the model reasonably well suggests that the model may be useful for the third row and that the intrinsic metal-hydrogen bond energy is again close to 60 kcal/mol. Data for other ions are obviously needed in order to verify more precisely these periodic trends.

### Reaction Mechanism

*Scandium.* As shown in Table I,  $\text{Sc}^+$  produced by SI is primarily in the ground state,  $^3\text{D}$  (88.6%) with smaller amounts of the first two excited states,  $^1\text{D}$  (6.0%) and  $^3\text{F}$  (5.4%). For  $\text{Sc}^+(\text{SI})$ , it is unlikely that a large portion of the observed reactivity is due to excited states simply because the cross section is of moderate size<sup>32</sup> and the excited states make up only a small portion ( $\approx 11\%$ ) of the beam. Also, the fact that the cross section peaks near 4.5 eV rather than earlier suggests that reaction is predominantly due to the ground state. Diabatically, the  $^3\text{D}(\text{sd})$  ground state is expected to react inefficiently in an impulsive manner, producing more  $\text{ScD}^+$  than  $\text{ScH}^+$  in the HD reaction. This is clearly inconsistent with the experimental reaction cross sections (Figure 4). Adiabatically, the  $^3\text{D}(\text{sd})$  state mixes with the  $^3\text{F}(\text{d}^2)$  state of  $\text{Sc}^+$ . This latter state should insert into HD and produce a near 1:1 ratio of  $\text{ScH}^+$  to  $\text{ScD}^+$  in the threshold region. This is more consistent with the observed reaction behavior of  $\text{Sc}^+$ .

The isotope ratio ( $\text{ScH}^+:\text{ScD}^+$ ) is still significantly larger than the statistical 1:1 ratio. This can be explained by noting that, of the five surfaces evolving from  $\text{Sc}^+(^3\text{D})$ , only three of them should behave statistically because they avoid populating the 4*s* and 3*d* $\sigma$  orbitals while populating the in-plane 3*d* $\pi(1b_2)$  orbital. The other two surfaces may react via more direct pathways, which should yield  $\text{ScH}^+$  preferentially. Another contributing factor may be

(30) Armentrout, P. B.; Georgiadis, R. *Polyhedron* **1988**, *7*, 1573-1581, and references therein.

(31) The correlation between the  $\text{MH}^+$  bond energy and the metal ion promotion energies given in ref 30 indicates that the  $\text{M}^+-\text{H}$  bond can be estimated by taking the intrinsic bond energy minus 0.51 times the promotion energy for the first row and 0.35 times the promotion energy for the second row. For this discussion, we assume that the third-row correlation is the same as for the second row. The data in Table I indicates that  $E_p$  is 3.8, 6.4, 5.9, and 43.6 kcal/mol for  $\text{Sc}^+, \text{Y}^+, \text{La}^+,$  and  $\text{Lu}^+$ , respectively.

(32) The cross section is larger than the cross sections for the ground states of  $\text{Ti}^+-\text{Fe}^+$ .<sup>1</sup> Comparisons with phase space theory calculations suggest that approximately one-fifth of the  $\text{Sc}^+$  ions are on "reactive" surfaces, while the remainder do not react. For comparison, Rappe and Upton<sup>8</sup> predict that three of the five ground-state components can contribute to the cross section via a perpendicular interaction while all five contribute if they react in a collinear fashion. Intermediate geometries may give different reaction probabilities.

(26) Elkind, J. L.; Armentrout, P. B. *Inorg. Chem.* **1986**, *25*, 1078-1080.

(27) Alvarado-Swaigood, A. E.; Harrison, J. F. *J. Phys. Chem.* **1985**, *89*, 5198-5202.

(28) Anglada, J.; Bruna, P. J.; Peyerimhoff, S. D.; Bunker, R. J. *J. Mol. Struct.* **1983**, *93*, 299-308.

(29) Schilling, J. B.; Goddard, W. A.; Beauchamp, J. L. *J. Am. Chem. Soc.* **1987**, *109*, 5565-5573.

the participation of the remaining excited state,  $^1D$ , which should react in a direct fashion and produce 3–4 times as much  $ScH^+$  as  $ScD^+$  in the threshold region of the HD reaction. The population is a mere 6%, but these low-spin states can be  $\approx 3$  times more reactive than the high spin states.<sup>7,15</sup>

**Yttrium.** From Table I, the ground state of  $Y^+$  is a  $^1S(s^2)$  state, but due to the presence of very low lying electronic states and the small multiplicity of the ground state, it represents only about 11% of the beam produced by SI at 2200 K. The dominant component (81%) of the SI beam is the  $^3D(sd)$  first excited state with a 7% contribution from the  $^1D(sd)$  second excited state. This means that the constitution of the  $Y^+$  beam is similar to that of  $Sc^+$ . For the  $YH^+$  product ion, the states are not the same as for  $ScH^+$ , a result of different atomic metal ion state energies. The ground state is  $^2\Sigma^+$ , with  $^2\Delta$  and  $^2\Pi$  states higher by 0.37 and 0.66 eV, respectively.<sup>10,29</sup> The orderings of the reactant and product states show that the s orbital is lower in energy than the d orbital by a larger amount in the case of  $Y^+$  than in the case of  $Sc^+$ . Overall, the MO correlations shown in Figure 1 are still qualitatively correct for the  $Y^+$  case.

The rather large reaction cross section measured makes it likely that a majority of the observed  $Y^+$  reaction is due to the  $^3D$  state. The ratio of  $YH^+$  to  $YD^+$  in the threshold of the HD reaction is  $\approx 1.4$ , and for the same reasons discussed above for the  $Sc^+$  system, we believe that the reaction is proceeding on a surface characteristic of the  $^3F(d^2)$  state of  $Y^+$ . We therefore conclude that most of the observed reaction is due to ions that originate on the repulsive  $Y^+(^3D) + H_2$  surface and insert by avoiding a crossing with the  $Y^+(^3F) + H_2$  diabatic surface.

Diabatically, the  $^1S$  state should react very inefficiently because of the doubly occupied s orbital. However, it should cross and mix with the low-lying  $^1D(sd)$  state. The 11% ground-state population and the 7% population of  $^1D$  ions in the  $Y^+(SI)$  beam should react in a direct fashion efficiently and raise the isotope ratio of the HD reaction. Thus, the  $Y^+$  system behaves very much the same as the  $Sc^+$  system, even though the low-lying electronic states are scrambled relative to one another.

**Lanthanum.** For  $La^+(SI)$ , the ground state is now  $^3F(d^2)$  and constitutes 69% of the SI beam. Smaller amounts of the low-lying  $^1D(sd)$ , 12%, and  $^3D(sd)$ , 15%, states are also present. Although calculations have not been performed on the low-lying states of  $LaH^+$ , the fact that the lowest state of  $La^+$  is a  $d^2$  rather than an  $s^2$  state suggests that the ordering will be similar to that for  $ScH^+(^2\Delta < ^2\Pi < ^2\Sigma^+)$ , with perhaps even larger spacing. Unlike  $Sc^+$  and  $Y^+$ , the d orbitals on  $La^+$  are lower in energy than the s orbital. Thus, the  $^3D(sd)$  surfaces will not cross those of the  $^3F(d^2)$ . We thus expect *diabatic* reactivity to predominate for these states. For the  $^1D(sd)$  state, however, there can still be a crossing with a  $d^2$  surface since any singlet  $d^2$  states lie higher in energy than the  $^1D(sd)$  state. Thus, the reactivity of  $La^+(^1D)$  could be diabatic (direct behavior) or adiabatic (insertion).

Again, the large size of the reaction cross section measured for  $La^+$  suggests that reaction is due primarily to the ground-state ion. The  $d^2$  ground state is expected to react diabatically and insert into HD to produce a statistical (1:1) distribution of products. This system comes very close to exhibiting this predicted behavior. We also note that the overall reaction cross section is markedly larger for  $La^+(SI)$  than for  $Sc^+(SI)$  and  $Y^+(SI)$ . This may indicate that the surface hopping between the  $^3D$  and  $^3F$  surfaces that must occur for  $Sc^+$  and  $Y^+$  is not perfectly efficient.  $La^+(SI)$  is more reactive since no surface crossing is required for the reaction. Furthermore, in the  $La^+$  system, SI produces more (13%) of the low-spin  $^1D(sd)$  state than in the  $Sc^+$  and  $Y^+$  systems. Since the branching ratio in the HD reaction indicates statistical behavior, this implies that if  $La^+(^1D)$  is contributing to the observed reactivity, then it is reacting primarily via an adiabatic pathway.

**Lutetium.** The  $Lu^+(SI)$  system is rather different from the other three systems in several respects. SI produces a beam of essentially pure (99.8%) ground-state  $^1S(s^2)$  because the  $^3D(sd)$  first excited state of  $Lu^+$  is comparatively high lying, at 1.63 eV. This is the first reaction system to provide us with a transition-metal ion beam that is nearly pure  $^1S$ . This clearly indicates that, for this system, the s orbital is lower in energy than the d orbitals such that Figure 1 is again qualitatively correct. Further, this state ordering implies that the  $^2\Sigma^+$  state of  $LuH^+$  is the ground state, as with  $YH^+$ . Indeed, other states of  $LuH^+$  are probably much higher in energy. The  $^1S$  state of  $Lu^+$  should correlate adiabatically with the  $LuH^+(^2\Sigma^+)$  state.

The diabatic behavior of the  $s^2$  state should be a strongly repulsive interaction since the MO considerations place two electrons into the antibonding  $4a_1^*$  orbital. However, this surface may undergo an avoided crossing with a surface evolving from the  $^1D(sd)$  state, 2.15 eV above the ground state. This state is expected to react primarily via a direct process. What we observe is that the excitation function for the reaction of  $Lu^+(SI)$  with  $D_2$  rises slowly and peaks late. In addition, in the reaction with HD, formation of  $LuD^+$  at threshold is favored over formation of  $LuH^+$  and the cross section for  $LuD^+$  has a lower apparent threshold. At higher energy, formation of  $LuH^+$  is favored by roughly 4:1 over  $LuD^+$ . The low-energy effect is unmistakably due to an impulsive mechanism,<sup>1,15</sup> while the high-energy behavior is indicative of a direct reaction mechanism.

What is apparently occurring in this system is an inefficient, impulsive reaction of  $Lu^+(^1S)$  at low energies, and then at higher energies, adiabatic behavior becomes more efficient and reaction switches to the  $Lu^+(^1D)$  surface. The switch to adiabatic behavior presumably does not occur at low energies due to the large separation of the  $^1S$  and  $^1D$  states of  $Lu^+$ , 2.15 eV. This is easily the largest asymptotic energy difference in reactions where avoided crossings have been invoked to explain the observed reactivity.

## Conclusions

Analysis of the reactions of  $M^+$  ( $M = Sc, Y, La,$  and  $Lu$ ) give the 0 K thermochemical values  $D^\circ(Sc^+-H) = 2.44 \pm 0.09$  eV ( $56.3 \pm 2.1$  kcal/mol),  $D^\circ(Y^+-H) = 2.66 \pm 0.06$  eV ( $61.3 \pm 1.4$  kcal/mol),  $D^\circ(La^+-H) = 2.48 \pm 0.09$  eV ( $57.2 \pm 2.1$  kcal/mol), and the more tentative value,  $D^\circ(Lu^+-H) = 2.11 \pm 0.16$  eV ( $48.6 \pm 3.7$  kcal/mol). The data are in reasonable agreement with the bond energies expected on the basis of the metal ion promotion energies<sup>30</sup> and suggest that the intrinsic bond energy for the third row is  $\approx 60$  kcal/mol.

The *diabatic* reactivity rules developed previously for the first-row transition-metal elements do not hold for the group 3 elements. This is consistent with the existence of surface crossings that are avoided, leading to adiabatic reactivity.  $Sc^+$ ,  $Y^+$ , and  $La^+$  are seen to react primarily via insertion, while  $Lu^+$  reacts via an impulsive mechanism at threshold and via a direct reaction at higher energies.  $Sc^+$ ,  $Y^+$ , and  $Lu^+$  show adiabatic behavior, with crossings from potential energy surfaces derived from  $s^2$  and  $sd$  configurations to more reactive surfaces derived from  $d^2$  configurations ( $Sc$  and  $Y$ ) or  $sd$  configurations ( $Lu$ ). For  $La^+$ , diabatic reaction along a  $d^2$  surface explains the bulk of the reactivity. Basically, the lowest energy pathway of a given spin state is followed. There is no need to invoke crossings between singlet and triplet surfaces, although such interactions cannot be ruled out.

**Acknowledgment.** This work is supported by the National Science Foundation, Grant CHE-8796289, and a National Science Foundation Graduate Fellowship (L.S.S.).

**Registry No.**  $Sc^+$ , 14336-93-7;  $Y^+$ , 14782-34-4;  $La^+$ , 14175-57-6;  $Lu^+$ , 16887-05-1;  $H_2$ , 1333-74-0;  $D_2$ , 7782-39-0; HD, 13983-20-5.